2013

The effect of sulfur covalent bonding on the electronic shells of silver clusters

Anthony F. Pedicini
Virginia Commonwealth University, pediciniaf@vcu.edu

Arthur C. Reber
Virginia Commonwealth University, acreber@vcu.edu

Shiv N. Khanna
Virginia Commonwealth University, snkhanna@vcu.edu

Pedicini, A. F., Reber, A. C., & Khanna, S. N. The effect of sulfur covalent bonding on the electronic shells of silver clusters. The Journal of Chemical Physics, 139, 164317 (2013).

The effect of sulfur covalent bonding on the electronic shells of silver clusters

Anthony F. Pedicini, Arthur C. Reber, and Shiv N. Khanna[a)]
Department of Physics, Virginia Commonwealth University, Richmond, Virginia 23284, USA

(Received 25 August 2013; accepted 13 October 2013; published online 30 October 2013)

The nature of the bonding in $Ag_nS_m^{0/-}$ clusters, $n = 1$–7; $m = 1$–4, has been analyzed to understand its effect on the electronic shell structure of silver clusters. First-principle investigations reveal that the sulfur atoms prefer 2 or 3-coordinate sites around a silver core, and that the addition of sulfur makes the planar structures compact. Molecular orbital analysis finds that the $3p$ orbitals of sulfur form a bonding orbital and two weakly bonding lone pairs with silver. We examine the electronic shell structures of Ag_6S_m, which are two electrons deficient of a spherical closed electronic shell prior to the addition of sulfur, and $Ag_7S_m^-$ clusters that contain closed electronic shells prior to the addition of sulfur. The Ag_6S_4 cluster has a distorted octahedral silver core and an open shell with a multiplicity of 3, while the $Ag_7S_n^-$ clusters have compact geometries with enhanced stability, confirming that the clusters maintain their electronic shell structure after bonding with sulfur. [http://dx.doi.org/10.1063/1.4827091]

I. INTRODUCTION

Noble metal particles have always attracted attention, largely due to their optical properties and it was almost 150 years ago that Faraday synthesized and demonstrated the colors of colloidal gold.[1] The properties of this new state of matter have been found to be very different from the bulk and the synthesis of materials using selected clusters as the building blocks is a promising strategy for the design of new materials with desired characteristics.[2] Metallic clusters, however, generally coalesce when assembled as bare entities and one needs ways to protect the individual clusters. One of the successful approaches to stabilize the new materials is to attach ligands that can prevent fusion of clusters as they are assembled.[3–8] This approach has been particularly successful for noble metal clusters, and numerous atom-precise clusters based ligated gold and silver particle assemblies have been synthesized.[9–20] Many of the ligands of choice use the sulfur containing thiol group and the passivation and stabilization of bare metallic clusters through the addition of thiols during synthesis also allows for the tuning of optical, physical, and electronic properties.[21–37] In addition to pure species, as we showed in a recent work, the ligation allows stabilization of cluster based material containing even a bimetallic core. The new material consisted of Ag_4Ni_2 clusters ligated with DMSA where the silver and the nickel atoms are linked by S atoms.[38]

The conceptual framework over which the cluster's stability may be understood is the superatom model which finds that clusters with a zero effective valence may be found when the number of itinerant valence electrons in the metallic core corresponds to an electronic shell closing.[39] This model has been quite successful in rationalizing the stability of bare and ligand protected clusters.[8,25,39] The silver (or gold) atoms provide one delocalized valence electron as the atomic configuration $4d^{10}\ 5s^1$ ($5d^{10}\ 6s^1$) where the d electrons are filled and the $5s$ are delocalized as a diffuse electron gas. The confined nearly free electron gas results in electronic states that are grouped into shells with effective quantum numbers in a spherical cluster of $1S^2$, $1P^6$, $1D^{10}$, $2S^2$ with corresponding magic numbers of 2, 8, 18, and 20.[40,41] These closed electronic shell structures have large HOMO-LUMO gaps, reduced reactivity with molecular oxygen, and enhanced stability.[42,43] For nonspherical metallic clusters, the electron gas undergoes a crystal field like splitting,[43–46] for example, Ag_6 has six valence electrons and a planar structure, so the $1P^6$ orbitals are split into two low lying $1P_x$ and $1P_y$ orbitals, and an unoccupied $1P_z$ orbital resulting in a large HOMO-LUMO gap. The addition of sulfur ligands reduces the effective valence electron count by moving a delocalized electron into a localized bonding orbital. To understand the fundamental principles underlying this model, we seek to understand the bonding between sulfur and noble metals and the effect of the bonding on the electronic shell structure of the noble metal cluster. To do this, we investigate the stability and reactivity of Ag_nS_m clusters as the simplest model system which may help develop such a base of knowledge.

The purpose of this paper is to present first principles theoretical studies on the atomic structure, electronic structure, and reactivity of neutral and anionic $Ag_nS_m^{0/-}$ clusters, $n = 1$–7; $m = 1$–4. In addition to the silver cluster based materials, our work is motivated by recent studies on the effect of sulfur on the stability of Ag nanoislands.[47] The studies indicate that the presence of sulfur enhances the coarsening of Ag nanoislands on Ag(100). An analysis of the experimental data suggests that AgS_2 cluster might be active for such a coarsening. Our studies on the stability of the cluster towards the removal of a Ag or S atom may be useful to develop a physical picture. We would like to add that the atomic and electronic structure of neutral and charged silver clusters Ag_n, Ag_n^-,

a)Author to whom correspondence should be addressed. Electronic mail: snkhanna@vcu.edu

and Ag_n^+ have attracted attention in several studies.[43,48–52] A recent study has also focused on the structure of $Ag_nS_4^-$ (n = 1–7) clusters that have been generated by the electrospray ionization of $Ag_7(DMSA)_4^-$, offering a mechanism for the production of $Ag_nS_n^-$ clusters.[51,53] There are several other studies on small AgS_m,[54] $Ag_{2n}S_n$,[55] and Au_nS^+ clusters.[56] However, a comprehensive investigation of the nature of the electronic structure modification of silver clusters through the addition of sulfur has yet to be explored. The present work is designed to fill this gap as it focuses on the electronic stability and properties of small silver–sulfur clusters through the sequential increases of Ag and incremental addition of S within Ag_nS_m and $Ag_nS_m^-$. In particular, we examine the electronic shell structures of Ag_6S_m, which are two electrons deficient of a spherical closed electronic shell prior to the addition of sulfur, and the $Ag_7S_m^-$ clusters that also contain closed electronic shells prior to addition of sulfur. This comparison reveals that the electronic shell structure of the silver clusters is still apparent after the addition of sulfur, and highlights the effect of bonding at the silver–sulfur interface.

II. THEORETICAL METHODS

First-principles electronic structure calculations on the neutral and anionic Ag_nS_m clusters were carried out within a gradient-corrected density-functional approach.[57] The electronic orbitals are represented by a linear combination of atomic orbitals that are formed, in turn, through a linear combination Slater-type orbitals (STO) located at the atomic sites. Actual calculations were completed using the Amsterdam Density Functional (ADF) set of codes.[58] To determine the ground state many initial geometries and spin multiplicities were sampled. All structures were fully optimized without constraint or symmetry to allow for full variational freedom. The clusters' molecular orbitals were assigned subshell distinctions through inspection of their nodes in the calculated wave function. The exchange and correlation effects were approximated using the gradient corrected functional proposed by Perdew, Burke, and Ernzerhof (PBE).[57] Relativistic effects were included using the Zeroth Order Regular Approximation[56] while employing a TZ2P basis and Large frozen electron core for both silver and sulfur atoms.

A fragmentation analysis as implemented within ADF was performed to get a deeper insight into the nature of the bonding.[58–60] In this analysis the system in question is considered as a sum of "fragments," each fragment yielding a basis set. The fragments are then combined to calculate the electronic structure of the full system. Here, we chose the silver cluster and the sulfur atoms themselves to serve as fragments. This procedure allows for both the analysis of the change in charge density within the cluster using the charge density of its composite fragments and also yields the requisite information needed in determining which orbitals are involved in bonding. Our calculated bond lengths for Ag–Ag, Ag–S, and S–S bonds are 2.60, 3.40, and 1.92 Å compared to the experimental values of 2.53 Å for the Silver dimer[61] and 1.89 Å for the Sulfur dimer, and no experimental result is available for AgS. The calculated bond strengths of 1.68 eV,[62] 2.40 eV, and 5.23 eV are also comparable to experimental values of 1.66 eV for Ag–Ag, and 4.40 eV for S–S bonds.

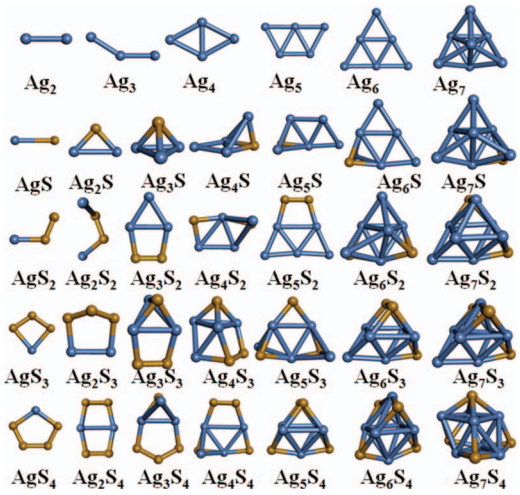

FIG. 1. Ground state geometries of neutral Ag_nS_m clusters, with n = 1–7 and m = 0–4.

III. RESULTS AND DISCUSSION

The ground state geometries of the neutral Ag_nS_m clusters are shown in Figure 1, and the anionic structures are shown in Figure 2. In all of the clusters with more than 3 silver atoms, the ground state structure is found to have a metallic center with all of the Ag atoms coordinated to one another, with sulfur binding at the periphery of the silver core. We are first interested in two features of the clusters: (1) how does the addition of sulfur affect the geometry of the silver core and (2) which sites of the silver cluster do the sulfur atoms prefer to bond? The Ag_n clusters are planar for n ≤ 6 atoms as is expected based on the electron count. For neutral Ag_nS_m clusters, the addition of sulfur leads to non-planar structure at smaller numbers of silver atoms than the Ag_n clusters. For example, the metallic cores in Ag_4S, Ag_5S, and Ag_6S are all nonplanar, with the sulfur displacing one silver atom from a

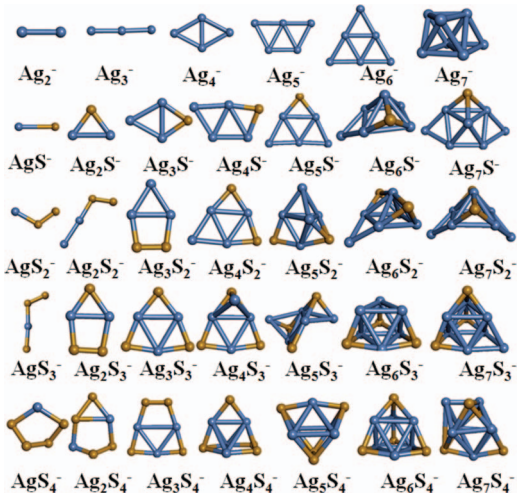

FIG. 2. Ground state geometries of $Ag_nS_m^-$ clusters, with n = 1–7 and m = 0–4.

planar geometry. The addition of successive sulfur eventually produces a compact metal core as seen in Ag_4S_3, Ag_5S_4, and Ag_6S_3. The Ag_7 cluster is essentially in a compact geometry for the pure cluster, so the addition of sulfur does not significantly compact the metallic core. The binding site of the sulfur for clusters with one or two silver atoms results in ring structures and sulfur-sulfur bonding; however, for clusters with more than three silver atoms, the predominant binding sites are the ones in which the sulfur atom binds to a 3-coordinated site with three silver atoms forming a distorted tetrahedron. There are a few cases of the sulfur forming a disulfide bond, in which adjacent sulfurs bind together, as seen in Ag_5S_2, Ag_5S_4, and Ag_6S_3. Of particular interest is the Ag_6S_4 cluster which has a structure in which the silver core forms a distorted octahedron, and the four sulfur atoms bind to 3-coordinated sites. The ground state structure of Ag_6S_4 is found to have a multiplicity of 3 corresponding to spin magnetic moment of 2 μ_b.

Figure 2 shows the ground state atomic structures of the anionic $Ag_nS_m^-$ clusters. The progression from planar to nonplanar silver core occurs with more sulfur atoms than the neutral clusters, however, the transition still occurs in all cases. The smallest non-planar clusters for $n = 4$, 5, and 6 are $Ag_4S_3^-$, $Ag_5S_2^-$, and Ag_6S^-. The metallic cores become compact with the additional sulfur, as seen in $Ag_4S_4^-$, $Ag_5S_4^-$, $Ag_6S_3^-$, and $Ag_7S_3^-$. There are several cases of the sulfur binding to the 2-coordinated sites on the edge of the metallic core; however, the most common binding site for the sulfur is the 3-coordinated site on top of three silver atoms. A disulfide bond is seen in $Ag_4S_4^-$ and $Ag_5S_4^-$. Of particular interest is the $Ag_7S_4^-$ cluster, as Ag_7^- has a closed electronic shell prior to the addition of sulfur, so the effect of the bonding of sulfur to a closed-shell cluster is especially intriguing.

To analyze the relative stability of the clusters, we next consider the removal energies (RE), the energy required to remove a single Ag or S atom from the cluster. These are calculated using the equation

$$\mathrm{RE} = \mathrm{E(A)} + \mathrm{E(A_{x-1}B_y)} - \mathrm{E(A_xB_y)}. \quad (1)$$

Here, E(A), $\mathrm{E(A_{x-1}B_y)}$, and $\mathrm{E(A_xB_y)}$ are the total energies of the A atom, $\mathrm{A_{x-1}B_y}$ cluster, and $\mathrm{A_xB_y}$ cluster, respectively. Figures 3(a) and 3(b) show the removal energy trends of Ag and S from the Ag_nS_m clusters. The silver removal energies of Figure 3(a) demonstrate an even-odd pattern for the Ag_n clusters, with Ag_6 showing the largest removal energy. The Ag_6S_m clusters exhibit enhanced Ag removal energies from $m = 0$–3 with the Ag_nS_4 series having its largest peak at Ag_5S_4. Note that Ag_6S_4 has a triplet ground state that probably causes this break in the trend. At smaller sizes, no clear trend emerges after the addition of two or more sulfur atoms. Figure 3(b) plots the S removal energy of the neutral clusters, which are consistently much larger than the silver removal energies due to the strong covalent bond between sulfur and silver. The binding of the sulfur atoms is seen to increase with additional silver atoms, with As_7S having the largest S removal energy and with AgS having the smallest. The binding of the second sulfur atom is generally larger than for the first sulfur atom except for Ag_2 and Ag_4, with the largest sulfur removal energy being at $m = 2$ for the AgS_m and Ag_7S_m clusters, 3 for

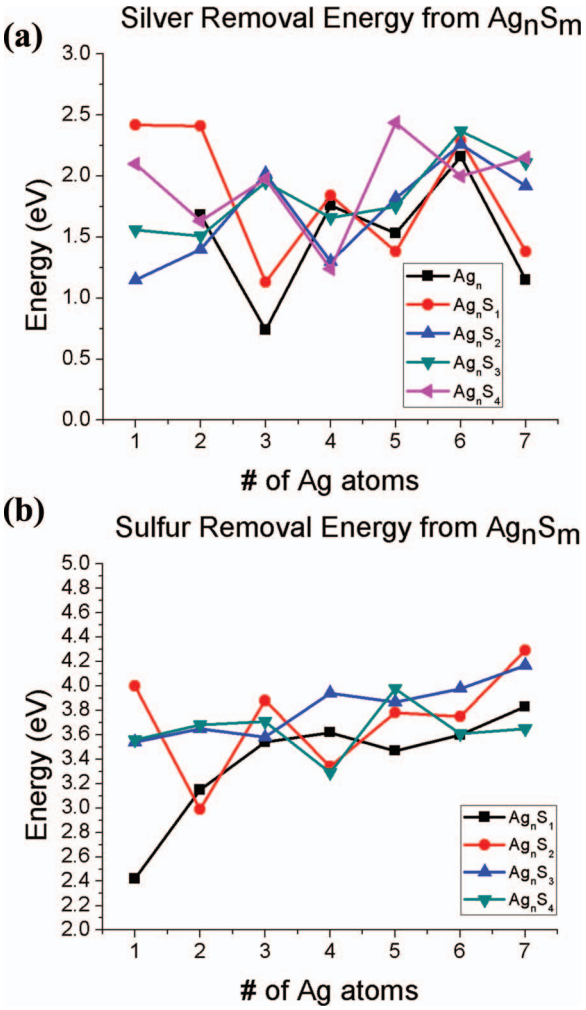

FIG. 3. Calculated removal energy plots for Ag (a) and S (b) in Ag_nS_m.

Ag_4S_m and Ag_6S_m, and 4 for Ag_2S_m and Ag_5S_m. The clusters of Ag_6S_m, which we have marked for particular interest shows that the S removal energy initially increases with the addition of S, and the S removal energy drops to its initial value with the addition of the fourth sulfur atom. This implies that the Ag_6S_m cluster series is becoming increasingly more stable through sulfur addition. As mentioned above, it has been suggested that a AgS_2 complex might be playing a role in the coarsening of Ag_n islands. The present study shows that this cluster has a low binding energy to remove a Ag atom while having a high energy to remove a S atom. The weak bonding of Ag seems consistent with the ability of S_2 to transport Ag atoms. However, further work, and inclusion of kinetics, is needed to examine this island formation.

We next analyze the removal energies for the anionic clusters $Ag_nS_m^-$ in Figures 4(a) and 4(b). An even-odd alternation in Ag removal energy for the Ag_n^- and Ag_nS^- series is seen in Figure 4(a), however for clusters with 2–4 sulfur atoms, the even-odd pattern is no longer apparent. This suggests that the bonding energy of the sulfur atom becomes more important to the stability of the cluster than the stabilization afforded by the shell closing of the metal cluster. The maximum silver removal energy for $m = 2$, 3, and 4 are found at $n = 7$, 6, and 5 respectively. The sulfur removal energies

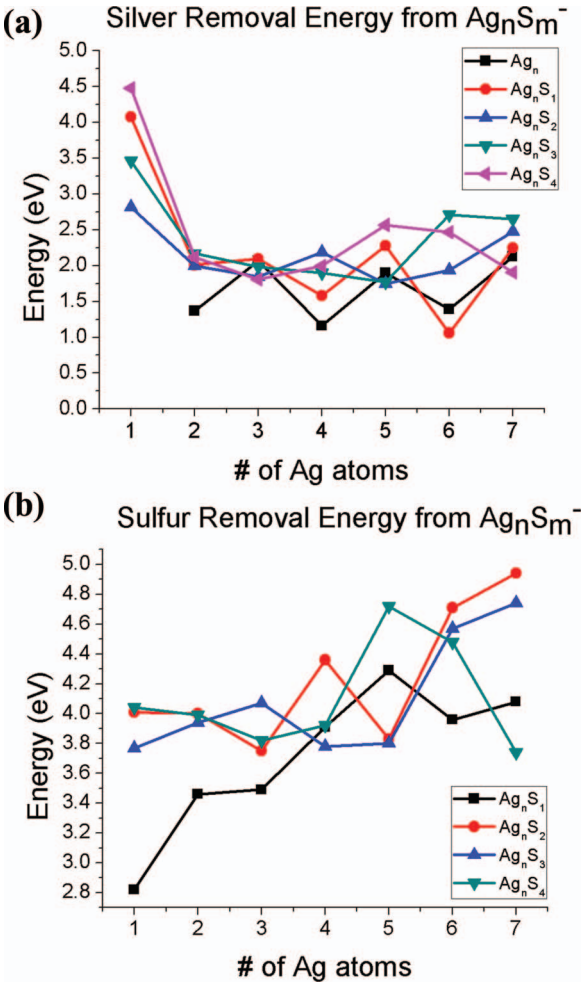

FIG. 4. Calculated removal energy plots for Ag (a) and S (b) in $Ag_nS_m^-$.

are shown in Figure 4(b), and it is seen that the addition of the second and third sulfur generally binds more strongly than the first sulfur, with the largest sulfur removal energy being $m = 2$ for the $Ag_2S_m^-$, $Ag_4S_m^-$, $Ag_6S_m^-$, and $Ag_7S_m^-$ clusters, 3 for $Ag_3S_m^-$, and 4 for AgS_m^- and $Ag_5S_m^-$. The largest sulfur binding energies are seen for $Ag_7S_2^-$ which is particularly surprising since Ag_7^- has a closed electronic shell, so one would expect it to bind sulfur most weakly. The electron affinities of the clusters are plotted in Figure 5, and show that these clusters are all quite stable as anions. The electron affinity increases with the addition of sulfur as the $m = 4$ Ag_nS_m clusters all have the highest electron affinity for a given number of sulfur atoms, and the $m = 0$ clusters all have the lowest electron affinity, except for Ag_3^-.

The HOMO-LUMO gaps of the neutral and anionic $Ag_nS_m^{0/-}$ clusters are plotted in Figures 6(a) and 6(b) to examine the effect of the sulfur on the electronic shell structure. Figure 6(a) shows that the largest HOMO-LUMO gaps for the Ag_n clusters are Ag_2 and Ag_6, as predicted by the nearly free electron model. The addition of sulfur decreases the HOMO-LUMO gap of nearly all of clusters, most notably in the Ag_6S_m clusters with the Ag_6 clusters having the largest gap and Ag_6S_4 having the smallest. We note that the Ag_6 cluster is expected to have a large gap with a planar structure,

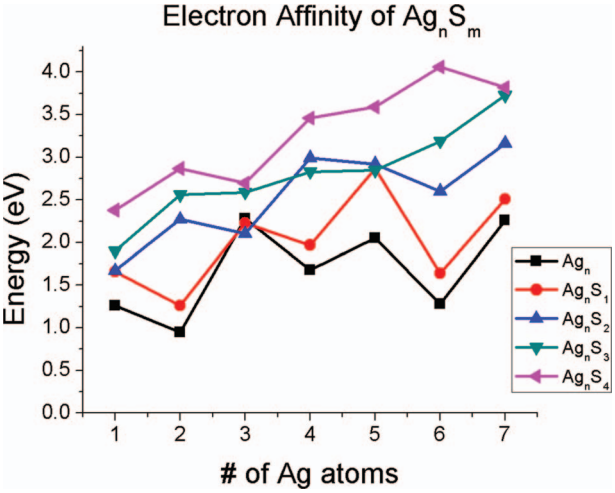

FIG. 5. Electron affinity (EA) of the Ag_nS_m clusters.

while both the Ag_6 cluster in an octahedral geometry and the Ag_6S_4 cluster which has a compact distorted octahedral structure have ground states with two unpaired electrons. If the sulfur was reducing the effective valence electron count of the cluster, the Ag_6S_4 would have an effective valence electron count of 2, which would result in a closed electronic shell. The

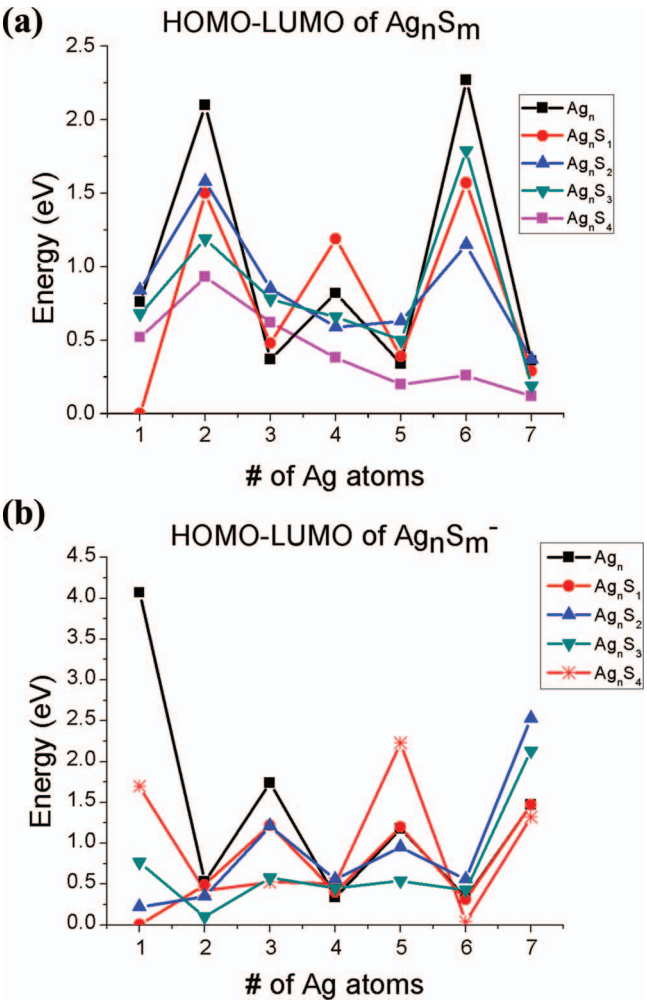

FIG. 6. Plot of the HOMO–LUMO gap energies of (a) netural Ag_nS_m and (b) anions.

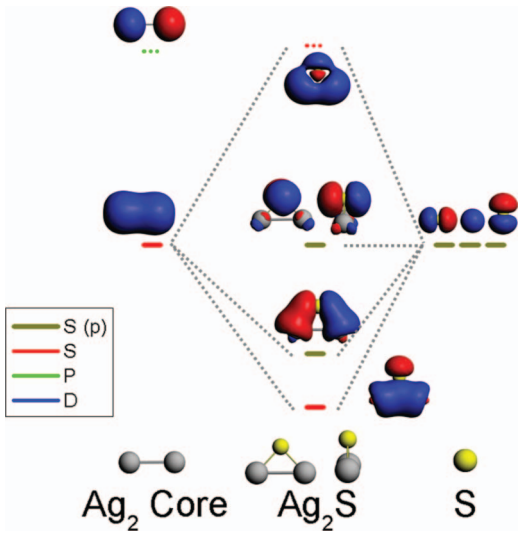

FIG. 7. One electron energy level schematic of the bonding between the Ag_2 and S atom form the Ag_2S cluster.

fact that the octahedral Ag_6S_4 cluster is maintaining the same spin multiplicity as the Ag_6 octahedral core suggests that the sulfur bonding is not disrupting the electronic shell structure of the Ag_6 core, although further analysis of the electronic structure is needed.

Figure 6(b) shows the HOMO-LUMO gaps of the $Ag_nS_m^-$ anions. Note that the unusually large gap of Ag^- distorts the scale as compared to Figure 6(a). An even odd oscillation is seen with the $Ag_5S_4^-$ having an especially large HOMO-LUMO gap, and the $Ag_7S_m^-$ series being of particular interest. Ag_7^- is interesting because its HOMO-LUMO gap is 1.47 eV, which is expected based on it having a closed electronic shell in the spherical jellium model with 8 valence electrons. The bonding with sulfur results in the Ag_7S^-, $Ag_7S_2^-$, and $Ag_7S_3^-$ all having the same or larger HOMO-LUMO gaps than Ag_7^-. $Ag_7S_4^-$ has a smaller gap than Ag_7^-, but it is still a respectable 1.32 eV. If the bonding with sulfur was reducing the effective valence electron count, then the HOMO-LUMO gap would decrease with the addition of sulfur. The HOMO-LUMO gaps indicate that the effect of sulfur bonding causes the HOMO-LUMO gap of the Ag_6S_m clusters to decrease while producing a compact metal core, while in the case of $Ag_7S_m^-$, the HOMO-LUMO gap is maintained.

Before we proceed further, let us examine the nature of bonding between Ag and S in detail by considering the electronic structure of the Ag_2S cluster, the simplest silver-sulfur cluster. Figure 7 shows the molecular orbital picture of Ag_2 and S combining to form Ag_2S. The Ag_2 has two valence electrons, and has a HOMO-LUMO gap of 2.10 eV. The addition of a single sulfur results in a structure in which the S binds in a 2-coordinated site to both silver atoms, also seen in Fig. 7. The Ag–Ag bond length expands from 2.60 Å in Ag_2 to 3.16 Å, and the HOMO-LUMO gap decreases to still a relatively large value of 1.50 eV. The sulfur 3*p* orbitals introduce three new orbitals, the lowest energy of which is a bonding orbital perpendicular to the surface of the cluster. The next lowest orbital is a more weakly bonding orbital where the 3*p* orbital of sulfur is parallel with the silver dimer, and the HOMO is a nonbonding orbital in which the 3*p* orbital of sulfur is perpendicular to the silver dimer. The LUMO is an antibonding orbital where the 3*p* orbital of sulfur is of opposite phase as the lowest energy valence orbital. The sulfur provides four valence electrons, and the Ag_2 provides two valence electrons. The overall shell structure of Ag_2 is still intact within Ag_2S, and the two orbitals of weakly bonded or lone pair primarily located on the sulfur are filled, becoming the frontier orbitals.

To understand the effect of sulfur on the electronic structure of Ag_6S_m and $Ag_7S_m^-$, their density of states along with their projected density of states is displayed in Figure 8. We also employ the tool of Overlap Population Density of States (OPDOS) in which a positive OPDOS points to constructive

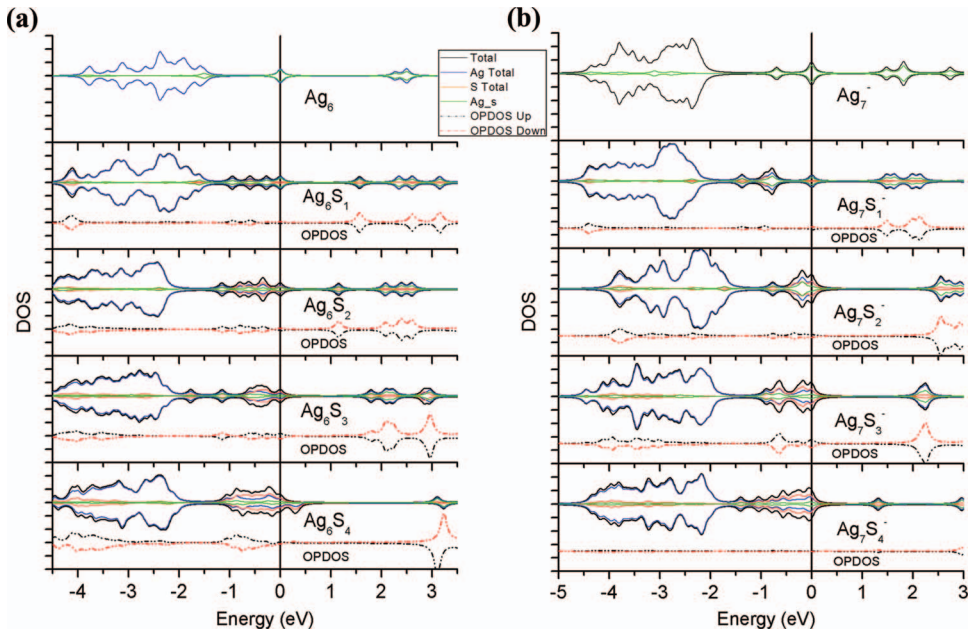

FIG. 8. Density of States, Projected Density of States, and OPDOS plots for Ag_6S_m (a) and $Ag_7S_m^-$ (b), $m = 0$–4.

interference between the Ag and S orbitals indicating covalent bonding, and a negative OPDOS points to destructive interference between the Ag and S orbitals indicating an antibonding orbital.[58,63] In our plots the black OPDOS is for the spin up channel, and the red in for the spin down, and the sign of the OPDOS has been inverted. In all plots, the 4*d* silver bands are prominent from −4.5 to −2.0 eV, while the green Ag 5*s* projected DOS indicate the delocalized orbitals are found mostly in the range of −2 to 0 eV. The sulfur states are most dense in this range as well, near the HOMO level, with some arising below the 4*d* band. Using the OPDOS plots we can verify that the sulfur density present below the 4*d* bands is bonding in nature, while the negative OPDOS of the LUMOs in all cases shows that they are antibonding. This is consistent with the molecular orbital plot from Figure 7, with one set of deep bonding orbitals appearing with a number of weakly bonding and nonbonding orbitals appearing at or near the HOMO. The presence of large density of 5*s* orbitals states also indicates that the delocalized orbitals of the metallic cluster are still occupied and are near the frontier orbitals. Another similarity between these densities of states and the simple picture in Ag_2S is that the LUMO of these clusters, except for Ag_6S_4, are all antibonding Ag-S orbitals. The density of states reveals two energy regions that are predominantly due to S, one deep in the energy spectrum, and a second near the HOMO, and that the LUMO of most of the Ag_nS_m clusters are antibonding orbitals between the silver and sulfur.

We next examine the molecular orbital diagrams of Ag_6S to examine the electronic structure. The top panel of Figure 9 shows the planar structure of Ag_6 and its large HOMO-LUMO gap of 2.27 eV. This gap size is explained by the structure of the cluster itself, which contains an electronic structure of delocalized Ag 5*s* states $|1S^2|1P^4\|1P^2|$, where capital letters represent the jellium-like delocalized orbital. This delocalized orbital representation also describes Ag_6S, where adding S to form Ag_6S result in two 1P orbitals, shown in green in Fig. 9, are still occupied. The sulfur provides one deep bonding orbital, and two lone-pair orbitals, but the electronic shell structure of the silver is still discernible.

The molecular orbital diagrams of Ag_6S_2, Ag_6S_3, and Ag_6S_4 are shown in the middle and bottom panels of Figure 9. We can see that both Ag_6S_2 and Ag_6S_3 have three molecular orbitals that can be assigned as 1P, resulting in the filling of the $1P^6$ shell. The fragment containing Ag_6 in the geometry of Ag_6S_2 has a near degeneracy at the HOMO, with a HOMO-LUMO gap of only 0.1 eV, and that the addition of S results in 3 lone pair orbitals for a total of 6 orbitals above the 4*d* band. Ag_6S_3 has a disulfide bond resulting in only 4 lone pair orbitals above the 4*d* band, as the disulfide bonding orbital is lower in energy.

The electronic structure of Ag_6S_4 has two unpaired electrons which result from having 11 orbitals above the 4*d* band, 3 of which correspond to the filling of the $1P^6$ shell, and 8 corresponding to the lone pair on sulfur. There are only 20 electrons available to fill these orbitals, and because the sulfur prefers to bind to a 3-coordinated site the cluster is unable to Jahn-Teller distort to quench its magnetic moment. The Ag_6 fragment in the geometry of Ag_6S_4 also has two unpaired electrons. This demonstrates that the metallic shell is still discernible is Ag_6S_4 even though the sulfur has bonded with the cluster.

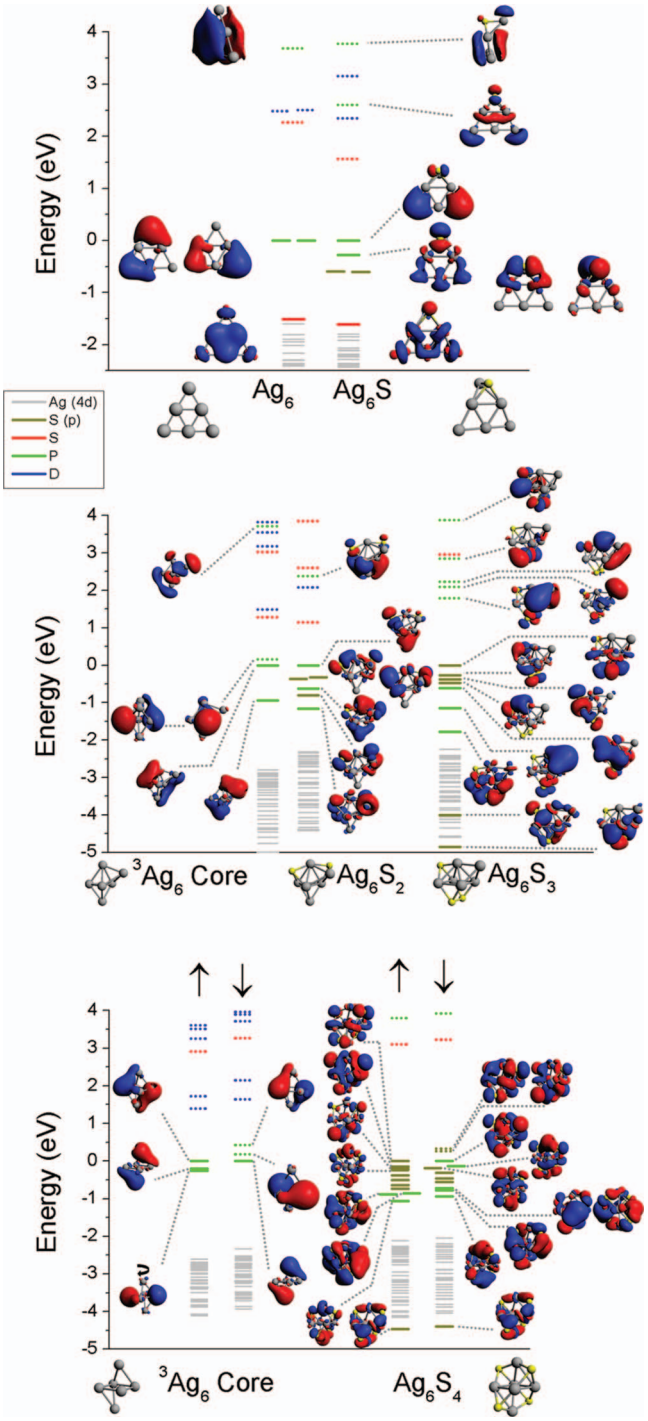

FIG. 9. The one electron energy levels and associated molecular orbital isosurfaces of Ag_6 & Ag_6S; $^3Ag_6$ Core, Ag_6S_2 & Ag_6S_3; $^3Ag_6$ Core & Ag_6S_4, arrows for spin-up and spin-down, respectively.

Next we examine the $Ag_7S_m^-$ clusters, where their pure cluster analogues already have a closed electronic shell. The top panel of Figure 10 shows the one electron levels of the Ag_7^- core belonging to the Ag_7S^- cluster. Surprisingly, the ground state structure results in an open metallic core in which the electronic shell structure is $1P^4$, with the $1P_z$ orbital antibonding in character with sulfur serving as the LUMO.

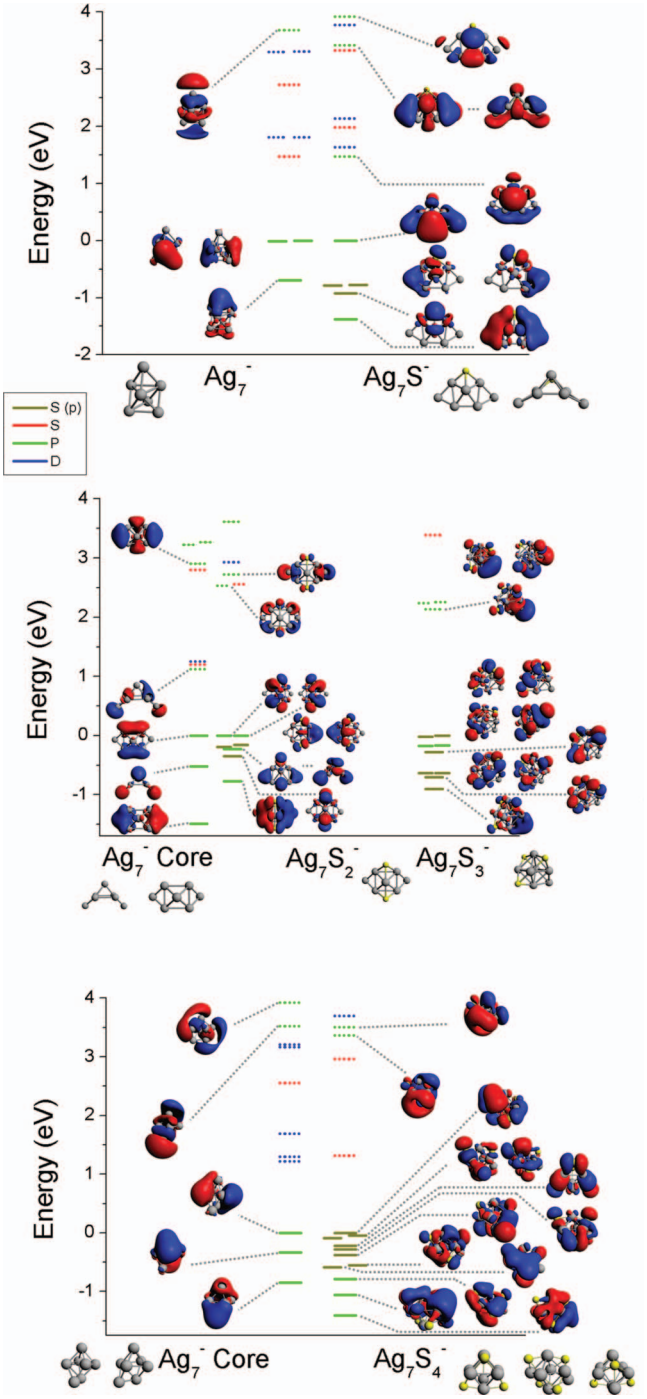

FIG. 10. The one electron energy levels and associated molecular orbital isosurfaces of Ag_7^- & Ag_7S^-; Ag_7^- Core, $Ag_7S_2^-$ & $Ag_7S_3^-$; Ag_7^- Core & $Ag_7S_4^-$.

The cluster still has 5 orbitals above the 4*d* band, so this may be due to one of the 1P orbitals hybridizing with the lone pair. For the $Ag_7S_2^-$ cluster and $Ag_7S_3^-$ cluster, as shown in Figure 10 (middle panel), the $1P^6$ shell is full in both the Ag_7^- cluster fragment and the $Ag_7S_2^-$ and $Ag_7S_3^-$ clusters. This shows that if the metallic core has a closed electronic shell, then the addition of sulfur maintains that closed shell character. The filled $|1P^6|$ orbital is also found in $Ag_7S_4^-$, with the electronic structure of the cluster above the 4*d* band consisting of 8 lone pair orbitals and 3 orbitals filling the $1P^6$ shell.

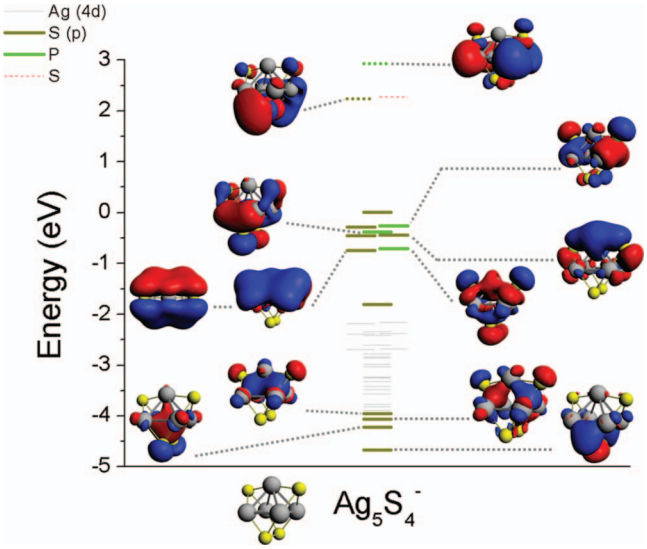

FIG. 11. The one electron energy levels and associated molecular orbital isosurfaces of $Ag_5S_4^-$.

This demonstrates that the bonding between sulfur and a silver cluster results in a deep bonding orbital per sulfur atom, and two weakly bonding/nonbonding orbitals per sulfur atom. Furthermore, the electronic shell structure of the Ag cluster is still discernible after the addition of the sulfur.

Lastly we examine the electronic structure of $Ag_5S_4^-$ because of its large 2.24 eV HOMO-LUMO gap, to understand the origin of its stability. The metallic core has a pyramidal structure, with two sulfurs decorating the faces of the pyramid, and two more forming a disulfide bond on the square face of the metallic core. The electronic structure reveals three deep bonding orbitals between the silver core and sulfur, a disulfide bond orbital, a filled $1P^6$ shell, and 6 lone pair orbitals. Figure 11 shows that the formation of the disulfide bond is due to two 3*p* sulfur orbitals perpendicular to the metal core, which reduces the number of lone pair orbitals. This offers another mechanism which affects the electronic structure. In some ways, this is more similar to the bonding of a sulfur based ligand, which will have one fewer lone pair orbitals per ligand than the atomic sulfur. The combination of a closed $1P^6$ shell, and a disulfide bond results in the $Ag_5S_4^-$ having a much larger HOMO-LUMO gap than any other of the $Ag_5S_m^-$ clusters.

IV. CONCLUSION

In summary, the geometric and electronic structures of neutral and anionic Ag_nS_m clusters have been investigated to understand the bonding and effect on the electronic shell structure of the silver core. It has been shown that the electronic shell structure of silver is maintained through subsequent additions of sulfur. This is demonstrated by the triplet multiplicity of the Ag_6S_4 cluster, in which the preferred 3-coordinate bonding site of sulfur results in the metallic core taking an octahedral structure. Because the bonding prevents a Jahn-Teller distortion from occurring, the cluster has the same triplet multiplicity of the Ag_6 cluster in an octahedral

structure. Secondly, the closed shell of Ag_7^- is retained after the addition of sulfur. Furthermore, one electron levels of the Ag_nS_m clusters have occupied orbitals that correspond to the filling of the $1P^6$ shells. A simple molecular orbital picture for the bonding of sulfur to the metallic core is found in which one bonding orbital and two lone-pair orbitals are formed for each sulfur added. The exception to this rule is the case of the disulfide bond, which results in the reduction of one in the number of lone pair orbitals. These results verify that electron counting rules with the addition of sulfur are still valid and indicate the metallic shell structure of silver clusters bound by sulfur is surprisingly robust.

ACKNOWLEDGMENTS

We gratefully acknowledge support from the Air Force Office of Scientific Research through Grant No. FA9550-12-1-0481.

[1]M. Faraday, Philos. Trans. R. Soc. London **147**, 145 (1857).
[2]S. Mandal, A. C. Reber, M. Qian, P. S. Weiss, S. N. Khanna, and A. Sen, "Controlling the band gap energy of cluster-assembled materials," Acc. Chem. Res. (published online).
[3]C. E. Briant, B. R. C. Theobald, J. W. White, L. K. Bell, D. M. P. Mingos, and A. J. Welch, J. Chem. Soc. Chem. Commun. **1981**, 201.
[4]P. D. Jadzinsky, G. Calero, C. J. Ackerson, D. A. Bushnell, and R. D. Kornberg, Science **318**, 430 (2007).
[5]Y. Shichibu, Y. Negishi, T. Watanabe, N. K. Chaki, H. Kawaguchi, and T. Tsukuda, J. Phys. Chem. C **111**, 7845 (2007).
[6]M. Zhu, C. M. Aikens, F. J. Hollander, G. C. Schatz, and R. Jin, J. Am. Chem. Soc. **130**, 5883 (2008).
[7]M. B. Abreu, C. Powell, A. C. Reber, and S. N. Khanna, J. Am. Chem. Soc. **134**, 20507 (2012).
[8]H. Häkkinen, Nat. Chem. **4**, 443 (2012).
[9]M. W. Heaven, A. Dass, P. S. White, K. M. Holt, and R. W. Murray, J. Am. Chem. Soc. **130**, 3754 (2008).
[10]D. E. Bergeron, O. Coskuner, J. W. Hudgens, and C. A. Gonzalez, J. Phys. Chem. C **112**, 12808 (2008).
[11]P. R. Nimmala and A. Dass, J. Am. Chem. Soc. **133**, 9175 (2011).
[12]H. Xiang, S.-H. Wei, and X. Gong, J. Am. Chem. Soc. **132**, 7355 (2010).
[13]A. Dass, J. Am. Chem. Soc. **131**, 11666 (2009).
[14]A. Dass, J. Am. Chem. Soc. **133**, 19259 (2011).
[15]Z. Wu, E. Lanni, W. Chen, M. E. Bier, D. Ly, and R. Jin, J. Am. Chem. Soc. **131**, 16672 (2009).
[16]G. Shafai, S. Hong, M. Bertino, and T. S. Rahman, J. Phys. Chem. C **113**, 12072 (2009).
[17]K. M. Harkness, Y. Tang, A. Dass, J. Pan, N. Kothalawala, V. J. Reddy, D. E. Cliffel, B. Demeler, F. Stellacci, O. M. Bakr, and J. A. McLean, Nanoscale **4**, 4269 (2012).
[18]D. Jiang, S. H. Overbury, and S. Dai, J. Am. Chem. Soc. **135**, 8786 (2013).
[19]H. Yang, Y. Wang, H. Huang, L. Gell, L. Lehtovaara, S. Malola, H. Häkkinen, and N. Zheng, Nat. Commun. **4**, 2422 (2013).
[20]H. Yang, J. Lee, B. Wu, Y. Wang, M. Zhou, A. Xia, and L. Zheng, Chem. Commun. **49**, 300 (2013)
[21]M. D. Malinsky, K. L. Kelly, G. C. Schatz, and R. P. Van Duyne, J. Am. Chem. Soc. **123**, 1471 (2001).
[22]H. Häkkinen, M. Walter, and H. Grönbeck, J. Phys. Chem. B **110**, 9927 (2006).
[23]Y. Yanagimoto, Y. Negishi, H. Fujihara, and T. Tsukuda, J. Phys. Chem. B **110**, 11611 (2006).
[24]U. Landman, B. Yoon, C. Zhang, U. Heiz, and M. Arenz, Top. Catal. **44**, 145 (2007).
[25]M. Walter, J. Akola, O. Lopez-Acevedo, P. D. Jadzinsky, G. Calero, C. J. Ackerson, R. L. Whetten, H. Grönbeck, and H. Häkkinen, Proc. Natl. Acad. Sci. U.S.A. **105**, 9157 (2008).
[26]K. Baishya, J. C. Idrobo, S. Öğüt, M. Yang, K. Jackson, and J. Jellinek, Phys. Rev. B **78**, 075439 (2008).
[27]C. Noguez and I. L. Garzón, Chem. Soc. Rev. **38**, 757 (2009).
[28]D. M. Alloway, A. L. Graham, X. Yang, A. Mudalige, R. Colorado, V. H. Wysocki, J. E. Pemberton, T. Randall Lee, R. J. Wysocki, and N. R. Armstrong, J. Phys. Chem. C **113**, 20328 (2009).
[29]I. Díez, M. Pusa, S. Kulmala, H. Jiang, A. Walther, A. S. Goldmann, A. H. E. Müller, O. Ikkala, and R. H. A. Ras, Angew. Chem., Int. Ed. **48**, 2122 (2009).
[30]O. M. Bakr, V. Amendola, C. M. Aikens, W. Wenseleers, R. Li, L. Dal Negro, G. C. Schatz, and F. Stellacci, Angew. Chem. **121**, 6035 (2009).
[31]O. Lopez-Acevedo, K. A. Kacprzak, J. Akola, and H. Häkkinen, Nat. Chem. **2**, 329 (2010).
[32]J. Akola, K. A. Kacprzak, O. Lopez-Acevedo, M. Walter, H. Grönbeck, and H. Häkkinen, J. Phys. Chem. C **114**, 15986 (2010).
[33]C. M. Aikens, J. Phys. Chem. Lett. **2**, 99 (2011).
[34]S. Malola and H. Häkkinen, J. Phys. Chem. Lett. **2**, 2316 (2011).
[35]P. A. Clayborne, O. Lopez-Acevedo, R. L. Whetten, H. Gronbeck, and H. Hakkinen, J. Chem. Phys. **135**, 094701 (2011).
[36]A. Dass, Nanoscale **4**, 2260 (2012).
[37]E. B. Guidez, V. Mäkinen, H. Häkkinen, and C. M. Aikens, J. Phys. Chem. C **116**, 20617 (2012).
[38]S. R. Biltek, S. Mandal, A. Sen, A. C. Reber, A. F. Pedicini, and S. N. Khanna, J. Am. Chem. Soc. **135**, 26 (2013).
[39]S. N. Khanna and P. Jena, Phys. Rev. B **51**, 13705 (1995).
[40]W. D. Knight, K. Clemenger, W. A. de Heer, W. A. Saunders, M. Y. Chou, and M. L. Cohen, Phys. Rev. Lett. **52**, 2141 (1984).
[41]M. Brack, Rev. Mod. Phys. **65**, 677 (1993).
[42]A. C. Reber, S. N. Khanna, P. J. Roach, W. H. Woodward, and A. W. Castleman, J. Am. Chem. Soc. **129**, 16098 (2007).
[43]Z. Luo, G. U. Gamboa, J. C. Smith, A. C. Reber, J. U. Reveles, S. N. Khanna, and A. W. Castleman, J. Am. Chem. Soc. **134**, 18973 (2012).
[44]K. Clemenger, Phys. Rev. B **32**, 1359 (1985).
[45]P. J. Roach, W. H. Woodward, A. C. Reber, S. N. Khanna, and A. W. Castleman, Phys. Rev. B **81**, 195404 (2010).
[46]Z. Luo, C. J. Grover, A. C. Reber, S. N. Khanna, and A. W. Castleman, J. Am. Chem. Soc. **135**, 4307 (2013).
[47]M. Shen, S. M. Russell, D.-J. Liu, and P. A. Thiel, J. Chem. Phys. **135**, 154701 (2011).
[48]A. C. Reber, G. U. Gamboa, and S. N. Khanna, J. Phys. Conf. Ser. **438**, 012002 (2013).
[49]M. Yang, K. A. Jackson, and J. Jellinek, J. Chem. Phys. **125**, 144308 (2006).
[50]R. Fournier, J. Chem. Phys. **115**, 2165 (2001).
[51]E. M. Fernández, J. M. Soler, I. L. Garzón, and L. C. Balbás, Phys. Rev. B **70**, 165403 (2004).
[52]J. Hagen, L. D. Socaciu, J. Le Roux, D. Popolan, T. M. Bernhardt, L. Wöste, R. Mitrić, H. Noack, and V. Bonačić-Koutecký, J. Am. Chem. Soc. **126**, 3442 (2004).
[53]Z. Wu, D. Jiang, E. Lanni, M. E. Bier, and R. Jin, J. Phys. Chem. Lett. **1**, 1423 (2010).
[54]P. Liu, C. Han, Z. Gao, F. Kong, and Q. Zhu, J. Phys. Chem. B **103**, 3337 (1999).
[55]A. A. Bagatur'yants, A. A. Safonov, H. Stoll, and H.-J. Werner, J. Chem. Phys. **109**, 3096 (1998).
[56]H. Woldeghebriel and A. Kshirsagar, J. Chem. Phys. **127**, 224708 (2007)
[57]J. P. Perdew, K. Burke, and M. Ernzerhof, Phys. Rev. Lett. **77**, 3865 (1996).
[58]G. te Velde, F. M. Bickelhaupt, E. J. Baerends, C. Fonseca Guerra, S. J. A. van Gisbergen, J. G. Snijders, and T. Ziegler, J. Comput. Chem. **22**, 931 (2001).
[59]E. van Lenthe, A. Ehlers, and E.-J. Baerends, J. Chem. Phys. **110**, 8943 (1999).
[60]W. H. Woodward, A. C. Reber, J. C. Smith, S. N. Khanna, and A. W. Castleman, J. Phys. Chem. C **117**, 7445 (2013).
[61]B. Simard, P. A. Hackett, A. M. James, and P. R. R. Langridge-Smith, Chem. Phys. Lett. **186**, 415 (1991).
[62]Q. Ran, R. W. Schmude, K. A. Gingerich, D. W. Wilhite, and J. E. Kingcade, J. Phys. Chem. **97**, 8535 (1993).
[63]T. Hughbanks and R. Hoffman, J. Am. Chem. Soc. **105**, 3528–3527 (1983).